Assessing the reversed exponential decay of the electrical conductance in molecular wires: The undeniable effect of static electron correlation

Sara Gil-Guerrero,[†] Ángeles Peña-Gallego,[†] Nicolás Ramos-Berdullas,[†,‡] Ángel Martín Pendás,[*,¶] and Marcos Mandado[*,†]

[†]*Department of Physical Chemistry, University of Vigo, Lagoas-Marcosende s/n, 36310, Vigo, Spain*

[‡]*Institute of Theoretical Chemistry, University of Vienna, Währinger Str. 17, 1090 Vienna, Austria*

[¶]*Department of Analytical and Physical Chemistry, University of Oviedo, Calle Julián Clavería 8, 33006, Oviedo, Spain*

E-mail: ampendas@uniovi.es; mandado@uvigo.es

Abstract

An extraordinary new family of molecular junctions, inaccurately referred to as "anti-Ohmic" wires in the recent literature, has been proposed based on theoretical predictions. The unusual electron transport observed for these systems, characterized by a reversed exponential decay of their electrical conductance, might revolutionize the design of molecular electronic devices. This behavior, which has been associated with intrinsic diradical nature, is reexamined in this work. Since the diradical character

arises from a near-degeneracy of the frontier orbitals, the employment of a multireference approach is mandatory. CASSCF calculations on a set of nanowires based on polycyclic aromatic hydrocarbons (PAHs) demonstrate that, in the frame of an appropriate multireference treatment, the ground state of these systems shows the expected exponential decay of the conductance. Interestingly, these calculations do evidence a reversed exponential decay of the conductance, although now in several excited states. Similar results have been obtained for other recently proposed candidates to "anti-Ohmic" wires. These findings open new horizons for possible applications in molecular electronics of these promising systems.

Keywords

anti-Ohmic, molecular junction, electron transport, multireference, diradical, topological insulator

Recent theoretical results in the field of molecular electronics have led to proposal of the existence of a new family of molecular nanowires with unusual properties, inaccurately referred to as "anti-Ohmic" systems.[1–22] The term Ohmic has been coined at macroscopic level, where for some materials, mainly metals, the current/voltage relation is linear, following the Ohm′s law. This proportionality is expected whenever the electrons' mean free path, usually determined by electron-phonon interactions, is much smaller than the sample's length. In this regime, the electrical conductance decays linearly with the length of the wire. Therefore, strictly speaking, wires constructed at molecular scale can be considered neither Ohmic nor anti-Ohmic. Normally, the charge transport efficiency of molecular wires, in which the electron transport is associated with non-resonant tunneling, decays exponentially with the length of the wire.[23–25]. However, the above-mentioned novel compounds evidence an unexpected behavior, as their conductance increases with length. Although this reversed exponential decay of the electrical conductance with the length of the wire was explored by different groups many years ago,[26–29] a subsequent work of Tada and Yoshizawa[15] on nano-sized graphite sheets has recently revived the interest for this topic. Despite theorists have subsequently proposed a large number of model systems with reversed exponential decay, no experimental evidence of this behavior has been yet found. However, experimental measurements of the electrical conductance in anthracene oligomers do not agree with theoretical predictions. For these wires, the exponential decay parameter, β, was found to be positive and the HOMO-LUMO energy gap in long wires significantly large.[30]

Two common characteristics have been established[2,14] for a system to follow this reversed behavior. First, most of the wires with efficient transport are proposed to be oligomers with strong π-orbital conjugation. Second, the increase of conductance has been connected with a significant diradical character or the contribution of zwitterionic forms[1,10,31], which in turn is related to a narrowing of the HOMO-LUMO gap. Both conditions are correlated, since the stabilization of the diradical structure is favored by aromaticity and a strong bond con-

jugation.

In a recent paper,[5] in which a set of quinoid systems were found to exhibit this reversed conductance/length behavior, an analogy was established between this character in molecular wires and the one-dimensional topological insulator (1D-TI) model of Su, Schrieffer and Heeger (SSH).[32] A chemical interpretation of 1D-TIs was recently proposed by Pendás *et al*[33] within the Hückel approach using polyacetylene as model. They demonstrated that, in 1D-TIs, the frontier orbitals are strongly localized at the edges, almost degenerated and far in energy from the valence and conduction bands, with the system being an insulator in the bulk and highly conducting at the edges. This is the case also for the quinoid structures,[5] which, as a paradigm of reversed exponential decay, exhibits all the properties associated with 1D-TIs at the molecular scale.

Once a consensus has been achieved about the crucial role that the narrowing of the HOMO-LUMO gap plays in the appearance of reverse exponential decay of the conductance, the sturdiness of the methodology employed by most authors in the field is to be questioned. As the frontier orbital energy gap decreases, a single-reference treatment is less and less appropriate reference for describing the system wavefunction, and recourse to multireference methods becomes mandatory, even if only a qualitatively correct treatment of the system is sought for. Although several authors have employed these methods to analyze the diradical character of the wires, these methodologies have not been extended to transmission calculations, wherein electron transport is almost invariably estimated by means of the Non-Equilibrium Green's Functions (NEGF) approach in combination with Density Functional Theory (DFT).[34,35] Exceptions to single-determinant methods are also found in the literature. For instance, Joachim et al. introduced the calculation of the electron transmission through the electron scattering matrix using a configuration interaction (CI) treatment.[36,37] This method is appropriate to analyze the effect of dynamic electron correlation, but not

enough to provide a satisfactory solution for systems with a very narrow HOMO-LUMO gap, where the static electron correlation is crucial. There have been also a number of efforts in the literature to address self-energy effects in the prediction of molecular conductance.[38,39] Again, being the effects we describe related to static, not dynamic correlation, they will no longer be discussed here. In this situation, multireference methods, such as Complete Active Space Self-Consistent Field (CASSCF) or Multireference Configuration Interaction (MRCI), are needed. Since preliminary CASSCF calculations on quinoid chains point to a complete quenching of the reverse exponential regime in the ground state, we believe that all the recently proposed candidates for "anti-Ohmic" behavior should be reviewed in light of these new results.[1]

According to this reasoning, a thorough study of some of these recently proposed systems is herein presented. In the body of this letter, we focus on nanowires based on polycyclic aromatic hydrocarbons (PAHs), comparing their conducting properties obtained from single- and multi-reference treatments. An equivalent analysis for some other proposed systems[2,14] is offered in the Supplementary Information (SI). These comprise molecular junctions formed by PAHs connected to gold leads by ethynylphenylthiol linkers, as well as cumulenes and quinoid-cumulenes moieties connected to gold by amine linkers. The conclusions reached for PAHs also hold for these other junctions.

Our results will prove that the orbital mixing and relaxation of occupied and virtual orbitals arising from the CASSCF treatment destroys the constructive interference that facilitate the electronic conduction in this type of molecular wires at DFT level. This does not depend a priori on the relative position of the Fermi level of the electrodes. The level alignment of the Fermi level will certainly change the relative value of the conductance for the different series of molecular wires investigated here, but it will not affect the conductance/length behavior within each series.

Firstly, carbon nanoribbons containing up to six fundamental units of naphthalene, anthracene, and tetracene were constructed following the scheme shown in Figure 1. The structures were optimized using DFT at the B3LYP/cc-pVDZ level, as implemented in the Gaussian 09 program.[40] Then the wavefunction stability was tested, finding that all the naphthalene structures from $n = 1$ to $n = 6$ units display a stable wavefunction. On the contrary, this is not the case in the anthracene- and tetracene-based systems, in which an instability unfolds for those structures with $n > 2$ and $n > 1$, respectively. Reoptimization of the unstable structures in the triplet state sheds light on the origin of the instabilities, as they arise whenever the singlet-triplet gap is either about to close or even inverted (see Tables S1 and S2 of the SI).

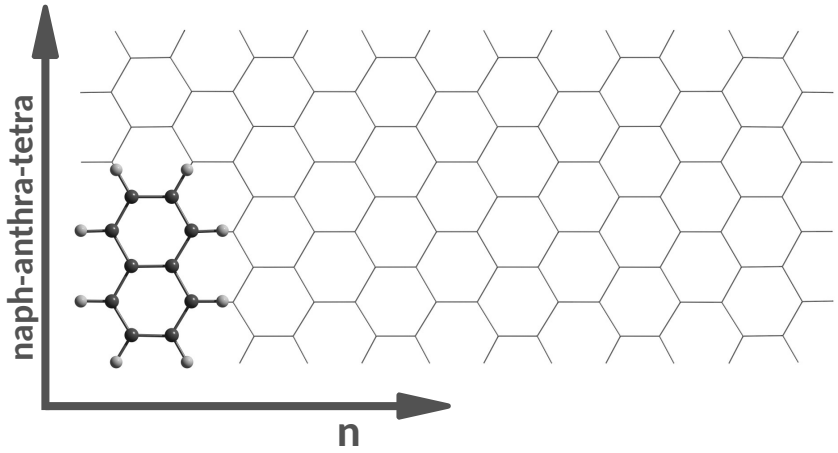

Figure 1: Schematic representation of the structure of the PAHs molecules studied in this work.

Given that multireference schemes are not yet available in standard NEGF-DFT implementations, an independent procedure able to extract the electrical conductance in molecular junctions at any level of theory is needed. In the context of the time-energy uncertainty approach, the electrical conductance can be explicitly obtained from electron transmission channels constructed from positive-negative pairs of Electron Deformation Orbitals (EDOs).[41] An in-house code (available upon request) has been used to the obtain conductance for all the

proposed systems under the application of a bias voltage of 2V. For all the molecular junctions whose results are included in the SI, the electron transmission was calculated within the NEGF-DFT approach and compared to the conductance obtained from EDOs. In all cases, the same trends are found (see SI, Figures S5, S6, S14 and S15). The electrical conductance G for the PAHs is represented in Figure 2. Clearly, G increases with the size of the fundamental unit (tetracene > anthracene > naphthalene). In the anthracene and tetracene cases, G also increases with the number of units, whereas in naphthalene the conductance remains almost constant with the chain length. It can be observed how the trends are similar to those observed by Tada *et al* in nanosized graphene sheets.[15] Unfortunately, and importantly, we remark that it is in those structures in which the conductance is larger where the above-mentioned wavefunction instabilities appear.

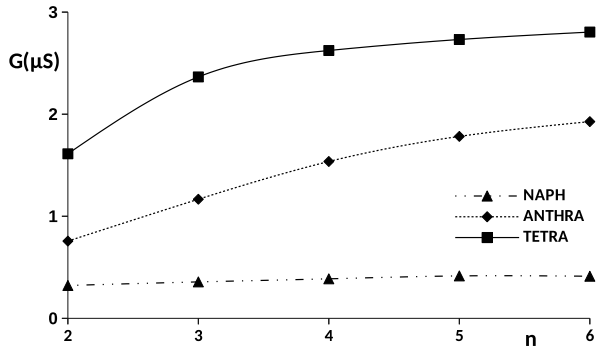

Figure 2: Evolution of the electrical conductance G, calculated within the EDOs formalism under a bias voltage of 2V, *vs* the number of fundamental units, n, in the PAHs.

As stated, reversed exponential decay is found in systems where frontier orbitals are almost degenerate and distant energetically from the valence and conduction bands. This is easily corroborated in Figure 3, where orbital bands are represented. One can observe that the energy gap closes as the system grows, and that this phenomenon arises at shorter lengths when the fundamental unit is larger. Thus, as expected, when the HOMO-LUMO near-degeneracy condition is reached, the band representation shows two isolated orbitals in the middle of the gap between the conductance and valence bands and, in turn, the fron-

tier orbitals become extremely localized at the edges of the molecule, as can be observed in Figures S1-S3 of the SI. There is an unequivocal connection between orbital localization and high conductance, but also with the instability of the wavefunction.

Orbital localization at the edges is also associated with a large long-range electron delocalization between them, and in turn to a strong electrical conductance. Martín Pendás *et al*[42] have shown how an atomic-pairwise additive partition of Resta's[43] localization tensor (LT) is intimately linked to electrical conductivity (see SI for further details). In molecular wires, the decay rate of the edge-to-edge component of the LT controls the overall G value, so that with a single descriptor, that can be computed both in single- and multi-reference frameworks, the conductance of a given system can be qualitatively estimated.[5]

Figure 4 contains the DFT values of the interatomic LT component computed between the carbon atoms located at right- and left-hand sides of the PAHs as represented in Figure 1. Results for $N = 1$, obtained between covalently linked atoms and thus unrelated to long-range delocalization effects, have not been included. It can be observed that naphthalene-based wires display a subtle decrease of their LT with the number of units, although the LT never vanishes. In contrast, the edge-to-edge LT of anthracene and tetracene wires shows a very clear divergence with n, characteristic of conductive behavior and in agreement with our estimations of conductance. This will be used as a clear evidence of reversed exponential decay.

We now consider the effect of the above-mentioned HOMO-LUMO near-degeneracy, as well as the wavefunction instability, on the overall DFT conductance picture. To that end we must shift to a multireference scenario. Single-point calculations of the ground state of the PAHs studied in this work were performed using the CASSCF method as implemented in MOLCAS.[44] We have employed both the simplest possible (2,2) space that involves exclusively the HOMO and LUMO orbitals, and an extended (14,14) one. The (2,2) space

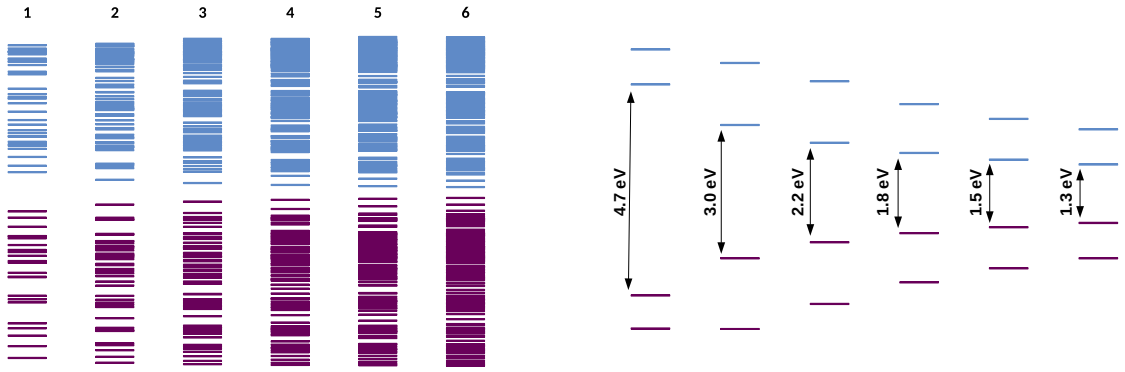

(a) Naphthalene

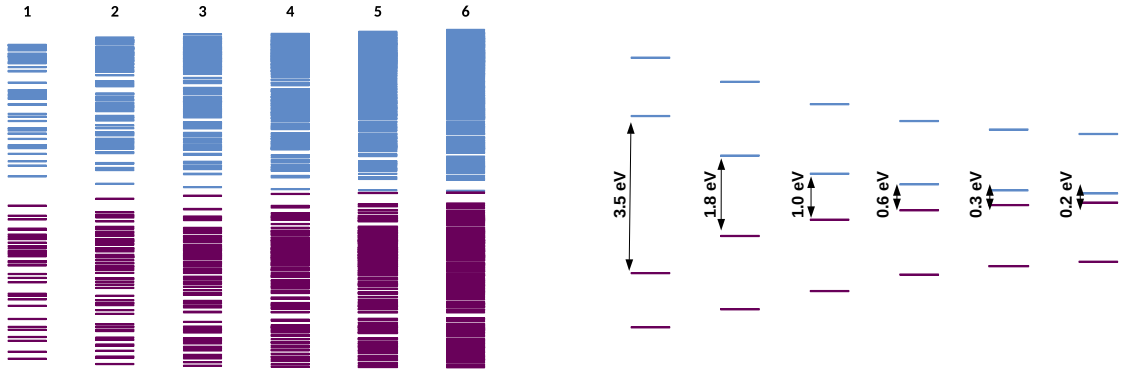

(b) Anthracene

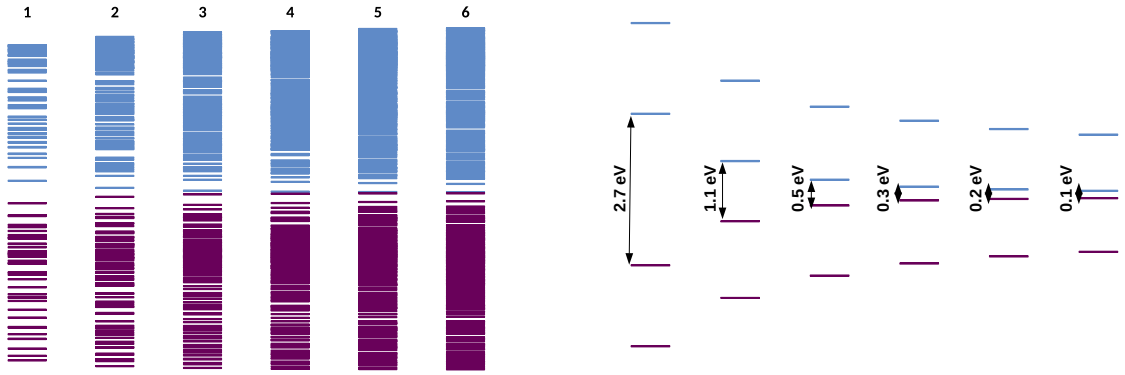

(c) Tetracene

Figure 3: Kohn-Sham orbital bands of the PAHs containing from $n = 1$ to $n = 6$ units within an energy window spanning of (-0.9)-(0.5) au range

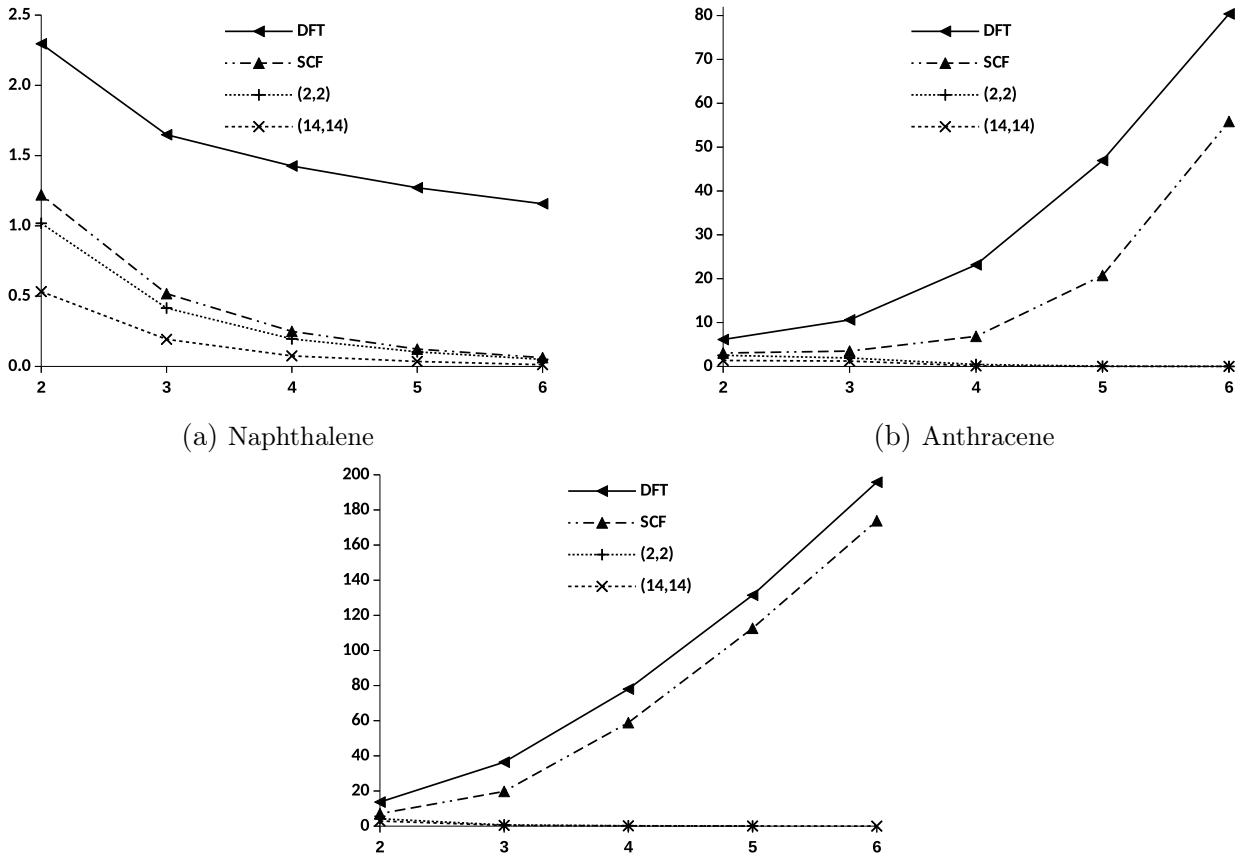

(a) Naphthalene

(b) Anthracene

(c) Tetracene

Figure 4: Evolution of the edge-to-edge interatomic localization tensor component (Λ^{AB}/au) *vs* the number of fundamental units, n, in the PAHs.

is a good choice for the largest systems, where the HOMO and LUMO are far from the remaining virtual and occupied orbitals. Also, for smaller systems, the choice of a (14,14) active space is accurate enough according to previous studies.[14] These calculations show that the ground state of the naphthalene-based structures is mainly represented by the doubly occupied HOMO configuration. However, for the anthracene and tetracene series, it can be observed that the doubly occupied LUMO configuration gains weight as the number of units increases, until reaching almost equal weight for the largest structures (see Tables S3 and S4 of the SI). In order to analyze the effect of these results in the conductance of the system, the LT was calculated with the SCF, CASSCF(2,2) and CASSCF(14,14) levels and represented in Figure 4. It can be observed that, for naphthalene, inclusion of static correlation does not

alter the qualitative single-determinant LT picture, although the LT decay is now considerably faster. However, for anthracene and tetracene, while the SCF calculations follow a curve that is less steep than in DFT, but still rising with the number of units, for the CASSCF calculations the LT drops to zero rapidly. As mentioned before, for the largest systems in both the anthracene and tetracene series, the LT results obtained using the (2,2) and (14,14) active spaces are basically coincident. These findings show not only that the single-reference treatment of the reversed exponential decay has been probably erroneous so far, but also that the physical properties obtained from single-reference modeling are misleading. When a proper methodology is used, our results suggest that the electrical conductance of the ground state of these systems follows the common exponential decay with length.

However, the multireference scenario raises the possibility of finding the reversed exponential decay, not in the ground but in an excited state. We are examining here the possibility that a multireference excited state well isolated from the ground state might display the appropriate coherence properties that we have shown to be destroyed by static correlation in the ground state. Such a state might be accessed, for instance, via an optical excitation. Once the excited state has been reached, the application of a bias voltage would further mix it with other states and allow for electrical conductance. In order to prove this statement, State Average calculations were performed in the tetracene structures, since it is in these cases in which the LT evidences the most notable differences between the single- and the multireference scenario for the ground state. The smallest (2,2) space is reasonable enough to describe the first two excited states in the series. Within this simplified description, three possible singlet spin-adapted states are accessible, coming from the doubly occupied HOMO configuration $|H\bar{H}| \equiv H^2$, the doubly occupied LUMO $|L\bar{L}| \equiv L^2$ one and, finally, from the equal, positive weight linear combination , $1/\sqrt{(}2)(|H\bar{L}| + |\bar{H}L|) \equiv HL$. It is well-known that for a 2-electron system the wavefunction may be expanded in Slater determinants constructed with natural spin orbitals.[45] The exact calculation of delocalization indices using

this form of the wavefunction was implemented previously.[46] Herein, we have employed the same methodology to calculate the LT within the 2-electron active space for the ground and excited states. The results are presented in Figure 5 and reflect the exponential decrease of the localization tensor with the number of tetracene units, previously discussed for the ground state (X), and the irregular increase in the case of the two excited states (S1 and S2) arising from the CASSCF(2,2) calculation. This irregular trend can be explained in the context of the change in the excited states along the tetracene series. The coefficients of the different configurations and the relative energies of the excited states are collected in Table S5 of the SI. In summary, the two excited states in the shortest systems are quite different and well-separated in energy, the lowest energy state (S1) corresponding to the singlet spin-adapted configuration HL, whereas the highest energy state (S2) corresponds to a combination of L^2 and H^2 with a significantly larger contribution from L^2. S2 follows the same trend as X for the structures with n =2 and n =3, whereas in S1 the LT is significantly larger and increases with n. For n =4, the nature of the excited states changes completely, becoming a combination of the three spin-adapted configurations and giving rise to quasi-degenerate states for $n \geq 4$. As it can be seen in Figure 5, the LTs of S1 and S2 become quite similar at n =4, and increase gradually for $n > 4$ with almost identical values for the two states. These results clearly indicate that large PAHs may display reversed exponential decay not in the ground state but in some of the lowest-energy excited states.

In conclusion, we believe that the results shown in this letter call into question the reversed exponential decay of the electrical conductance in molecular wires, at least in their ground state. We believe that the alleged exceptional electrical properties of recently proposed molecular systems have been predicted with methods that cannot tackle degeneracies or near degeneracies. In the context of a single-determinant procedure, such as that implemented in standard DFT, the electron transmission ability of these systems had already been linked with their diradical nature and to the vanishing of their HOMO-LUMO gap. In these

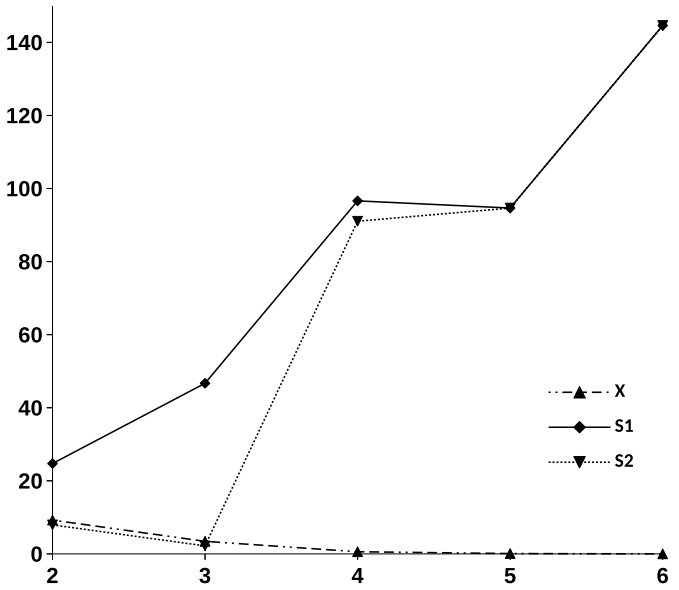

Figure 5: Evolution of the CASSCF(2,2) edge-to-edge interatomic localization tensor component (Λ^{AB}/au) *vs* the number of fundamental units, n, in the tetracene series. The first three singlet states are shown (X, S1, S2).

circumstances, multireference calculations should take over, and in fact they show that the diradical character leads to a normal exponential decay of the conductance with the length of the chain in ground states, although reversed exponential decay is still found, this time in low lying excited states. Our results warn against the blind use of standardized methods in the field of molecular electronics, while opening new avenues in fields like optoelectronics, where this type of wires might well have a chance to be experimentally proven.

Acknowledgements

S.G., A.P. and M.M. thanks Xunta de Galicia for financial support through the project GRC2019/24. N.R-B. thanks Xunta de Galicia for a postdoctoral grant. A.M.P. thank the spanish Ministerio de Ciencia, Innovación y Universidades for the grant PGC2018-095953-B-I00.

References

(1) Gil-Guerrero, S.; Ramos-Berdullas, N.; Mandado, M. *Org. Electron.* **2018**, *61*, 177–184.

(2) Garner, M. H.; Bro-Jørgensen, W.; Pedersen, P. D.; Solomon, G. C. *J. Phys. Chem. C* **2018**, *122*, 26777–26789.

(3) Algethami, N.; Sadeghi, H.; Sangtarash, S.; Lambert, C. J. *Nano Lett.* **2018**, *18*, 4482–4486.

(4) Chen, W.; Li, H.; Widawsky, J. R.; Appayee, C.; Venkataraman, L.; Breslow, R. *J. Am. Chem. Soc.* **2014**, *136*, 918–920.

(5) Gil-Guerrero, S.; Ramos-Berdullas, N.; Martín Pendás, Á.; Francisco, E.; Mandado, M. *Nanoscale Advances* **2019**, *1*, 1901–1913.

(6) Li, S.; Gan, C. K.; Son, Y.-W.; Feng, Y. P.; Quek, S. Y. *Carbon* **2014**, *76*, 285–291.

(7) Mahendran, A.; Gopinath, P.; Breslow, R. *Tetrahedron Lett.* **2015**, *56*, 4833–4835.

(8) Ramos-Berdullas, N.; Ferro-Costas, D.; Mandado, M. *Comput. Theor. Chem.* **2015**, *1053*, 263–269.

(9) Ramos-Berdullas, N.; Graña, A. M.; Mandado, M. *Theor. Chem. Acc.* **2015**, *134*, 20.

(10) Ramos-Berdullas, N.; Mandado, M. *Chem.: Eur. J.* **2013**, *19*, 3646–3654.

(11) Stuyver, T.; Fias, S.; De Proft, F.; Geerlings, P. *Chem. Phys. Lett.* **2015**, *630*, 51–56.

(12) Stuyver, T.; Fias, S.; De Proft, F.; Geerlings, P.; Tsuji, Y.; Hoffmann, R. *J. Chem. Phys.* **2017**, *146*, 092310.

(13) Stuyver, T.; Zeng, T.; Tsuji, Y.; Fias, S.; Geerlings, P.; De Proft, F. *J. Phys. Chem. C* **2018**, *122*, 3194–3200.

(14) Stuyver, T.; Zeng, T.; Tsuji, Y.; Geerlings, P.; De Proft, F. *Nano Lett.* **2018**, *18*, 7298–7304.

(15) Tada, T.; Yoshizawa, K. *J. Phys. Chem. B* **2004**, *108*, 7565–7572.

(16) Tsuji, Y.; Movassagh, R.; Datta, S.; Hoffmann, R. *ACS Nano* **2015**, *9*, 11109–11120.

(17) Valkenier, H.; Guédon, C. M.; Markussen, T.; Thygesen, K. S.; van der Molen, S. J.; Hummelen, J. C. *Phys. Chem. Chem. Phys.* **2014**, *16*, 653–662.

(18) Tada, T.; Yoshizawa, K. *Phys. Chem. Chem. Phys.* **2015**, *17*, 32099–32110.

(19) Sedghi, G.; Esdaile, L. J.; Anderson, H. L.; Martin, S.; Bethell, D.; Higgins, S. J.; Nichols, R. J. *Adv. Mater.* **2012**, *24*, 653–657.

(20) Li, Z.; Park, T.-H.; Rawson, J.; Therien, M. J.; Borguet, E. *Nano Lett.* **2012**, *12*, 2722–2727.

(21) Sedghi, G.; García-Suárez, V. M.; Esdaile, L. J.; Anderson, H. L.; Lambert, C. J.; Martín, S.; Bethell, D.; Higgins, S. J.; Elliott, M.; Bennett, N.; Macdonald, J. E.; Nichols, R. J. *Nat. Nanotechnol.* **2011**, *6*, 517–523.

(22) Sedghi, G.; Sawada, K.; Esdaile, L. J.; Hoffmann, M.; Anderson, H. L.; Bethell, D.; Haiss, W.; Higgins, S. J.; Nichols, R. J. *J. Am. Chem. Soc.* **2008**, *130*, 8582–8583.

(23) Winkler, J. R.; Gray, H. B. *J. Am. Chem. Soc.* **2014**, *136*, 2930–2939.

(24) McCreery, R. L.; Bergren, A. J. *Adv. Mater.* **2009**, *21*, 4303–4322.

(25) Ho Choi, S.; Kim, B.; Frisbie, C. D. *Science* **2008**, *320*, 1482–1486.

(26) Reimers, J.; Hush, N. *Chem. Phys.* **1989**, *134*, 323 – 354.

(27) Reimers, J.; Hush, N. *J. Photochem. Photobio. A* **1994**, *82*, 31 – 46.

(28) Joachim, C. *Chem. Phys.* **1987**, *116*, 339 – 349.

(29) Joachim, C.; Magoga, M. *Chem. Phys.* **2002**, *281*, 347 – 352.

(30) Koch, M.; Ample, F.; Joachim, C. H.; Grill, L. *Nat. Nanotechnol.* **2012**, *7 11*, 713–720.

(31) Morikawa, T.; Narita, S.; Klein, D. J. *Chem. Phys. Lett.* **2005**, *402*, 554–558.

(32) Su, W. P.; Schrieffer, J. R.; Heeger, A. J. *Phys. Rev. Lett.* **1979**, *42*, 1698–1701.

(33) Martín Pendás, Á.; Contreras-García, J.; Pinilla, F.; Mella, J. D.; Cárdenas, C.; Muñoz, F. A Chemical Theory of Topological Insulators. 28.01.2019; `https://chemrxiv.org/articles/A_Chemical_Theory_of_Topological_Insulators/7637009/1`.

(34) Herrmann, C.; Solomon, G. C.; Subotnik, J. E.; Mujica, V.; Ratner, M. A. *J. Chem. Phys.* **2010**, *132*, 024103.

(35) Deffner, M.; Gross, L.; Steenbock, T.; Voigt, B. A.; Solomon, G. C.; Herrmann, C. ARTAIOS - a transport code for postprocessing quantum chemical electronic structure calculations, available from https://www.chemie.uni-hamburg.de/ac/herrmann/software/index.html.

(36) Portais, M.; Joachim, C. *Chem. Phys. Lett.* **2014**, *592*, 272 – 276.

(37) Portais, M.; Hliwa, M.; Joachim, C. *Nanotechnology* **2016**, *27*, 034002.

(38) Strange, M.; Rostgaard, C.; Häkkinen, H.; Thygesen, K. S. *Phys. Rev. B* **2011**, *83*, 115108.

(39) Darancet, P.; Ferretti, A.; Mayou, D.; Olevano, V. *Phys. Rev. B* **2007**, *75*, 075102.

(40) Frisch, M. J.; Trucks, G. W.; Schlegel, H. B.; Scuseria, G. E.; Robb, M. A.; Cheeseman, J. R.; Scalmani, G.; Barone, V.; Petersson, G. A.; Nakatsuji, H.; et al., Gaussian 09. 2009.

(41) Ramos-Berdullas, N.; Gil-Guerrero, S.; Mandado, M. *Int. J. Quantum Chem.* **2018**, *118*, e25651.

(42) Pendás, Á. M.; Guevara-Vela, J. M.; Crespo, D. M.; Costales, A.; Francisco, E. *Phys. Chem. Chem. Phys.* **2017**, *19*, 1790–1797.

(43) Resta, R.; Sorella, S. *Phys. Rev. Lett.* **1999**, *82*, 370–373.

(44) Aquilante, F.; Autschbach, J.; Carlson, R. K.; Chibotaru, L. F.; Delcey, M. G.; De Vico, L.; Fdez. Galván, I.; Ferré, N.; Frutos, L. M.; Gagliardi, L.; et al., Open Molcas 8. *J. Comp. Chem.* **2015**, *37*, 506–541.

(45) Shull, H.; Löwdin, P. *J. Chem. Phys.* **1956**, *25*, 1035–1040.

(46) Mandado, M. *Theor. Chem. Acc.* **2013**, *132*, 1364.